

# Predictions of $p\bar{p}$ ; $p\bar{p}$ total cross section and ratio at LHC and cosmic-ray energies based on duality

Keiji Igi<sup>1</sup>, Muneyuki Ishida<sup>2</sup>

<sup>1</sup> Theoretical Physics Laboratory, RIKEN, Wako, Saitama 351-0198, Japan

<sup>2</sup> Department of Physics, Meisei University, Hino, Tokyo 191-8506, Japan

(Presented by Keiji Igi)

## Abstract

Based on duality, we previously proposed to use rich informations on  $p\bar{p}$  total cross sections below  $N$  ( $\sim 10$  GeV) in addition to high-energy data in order to discriminate whether these cross sections increase like  $\log$  or  $\log^2$  at high energies. We then arrived at the conclusion that our analysis prefers the  $\log^2$  behaviours. Using the FESR as a constraint for high energy parameters also for the  $p\bar{p}$ ,  $p\bar{p}$  scattering, we search for the simultaneous best fit to the data points of  $\sigma_{\text{tot}}$  and  $\sigma_{\text{ratio}}$  up to some energy (e.g., ISR, Tevatron) to determine the high-energy parameters. We then predict  $\sigma_{\text{tot}}$  and  $\sigma_{\text{ratio}}$  in the LHC and high-energy cosmic-ray regions. Using the data up to  $\sqrt{s} = 1.8$  TeV (Tevatron), we predict  $\sigma_{\text{tot}}^{\text{pp}}$  and  $\sigma_{\text{ratio}}^{\text{pp}}$  at the LHC energy ( $\sqrt{s} = 14$  TeV) as  $106.3 \pm 5.1_{\text{syst}} \pm 2.4_{\text{stat}}$  mb and  $0.126 \pm 0.007_{\text{syst}} \pm 0.004_{\text{stat}}$ , respectively. The predicted values of  $\sigma_{\text{tot}}$  in terms of the same parameters are in good agreement with the cosmic-ray experimental data sample up to  $P_{\text{lab}} = 10^8$  GeV by Block, Halzen and Stanov.

## 1 Introduction

As you all know, the sum of  $p\bar{p}$ ;  $p\bar{p}$  total cross sections has a tendency to increase above 70 GeV. It had not been known before 2002, however, if this increase behaved like  $\log$  or  $\log^2$  consistent with the Froissart-Martin bound [1]. So, we proposed [2] to use rich informations of  $p\bar{p}$  total

Invited talk given at "New Trends in High-Energy Physics" held at Yalta, Crimea (Ukraine), September 10-17, 2005.

cross sections at low energies in addition to high energy data in order to discriminate between asymptotic  $\log$  or  $\log^2$  behaviours, using a kind of the finite-energy sum rule (FESR) as constraints. Thus, duality is always satisfied in this approach.

Such a kind of attempt to investigate high-energy behaviours from those at low and intermediate energies has been initiated by one of the authors [3]. In the early days of the Regge pole theory, there were controversies if there are other singularities with the vacuum quantum numbers except for the Pomeron ( $P$ ). Under the assumption that no  $J$  singularities extend above  $J = 0$  except for the Pomeron, we were led to the exact sum rule [3] for the  $s$ -wave  $N$  scattering length  $a^{(+)}$  of the crossing-even amplitude as

$$1 + \frac{!}{M} a^{(+)} = \frac{f^2}{M} + \int_0^{\infty} dk \frac{^{(+)}}{\text{tot}}(k) \frac{^{(+)}}{\text{tot}}(1) - \frac{N}{M} : \quad (1)$$

The evidence that Eq. (1) was not satisfied empirically led to the  $P^0$  trajectory with  $P^0 = 0.5$  and the  $f$  meson with spin two was discovered on the  $P^0$  trajectory.

After 40 years, we have attempted [2] to investigate whether the  $p$  total cross sections increase like  $\log$  or  $\log^2$  at high energy based on the similar approach. We then arrived at the conclusion that our analysis prefers the  $\log^2$  behaviours consistent with the Froissart-Martin unitarity bound. Recently, Block and Halzen [4, 5] also reached the same conclusions based on duality arguments [6, 7].

## 2 General approach

Let us come to the main topics and begin by explaining how to predict  $\frac{^{(+)}}{\text{tot}}$ , the  $pp, pp$  total cross sections and  $\frac{^{(+)}}{\text{tot}}$ , the ratio of the real to imaginary part of the forward scattering amplitude at the LHC and the higher-energy cosmic-ray regions, using the experimental data for  $\frac{^{(+)}}{\text{tot}}$  and  $\frac{^{(+)}}{\text{tot}}$  for  $70 \text{ GeV} < P_{\text{lab}} < P_{\text{large}}$  as inputs. We first choose  $P_{\text{large}} = 2100 \text{ GeV}$  corresponding to ISR region ( $\sqrt{s} = 60 \text{ GeV}$ ). Secondly we choose  $P_{\text{large}} = 2 \times 10^6 \text{ GeV}$  corresponding to the Tevatron collider ( $\sqrt{s} = 2 \text{ TeV}$ ). Let us search for the simultaneous best fit of  $\frac{^{(+)}}{\text{tot}}$  and  $\frac{^{(+)}}{\text{tot}}$  in terms of high-energy parameters  $c_0, c_1, c_2$  and  $P^0$  constrained by the FESR. It turns out that the prediction of  $\frac{^{(+)}}{\text{tot}}$  agrees with  $pp$  experimental data at these cosmic-ray energy regions [8, 21] within errors in the first case (ISR). It has to be noted that the energy range of predicted  $\frac{^{(+)}}{\text{tot}}$ ,  $\frac{^{(+)}}{\text{tot}}$  is several orders of magnitude larger than the energy region of  $\frac{^{(+)}}{\text{tot}}$ ,  $\frac{^{(+)}}{\text{tot}}$  input (see Fig. 1). If we use data up to Tevatron (the second case), the

situation is much improved, although there are some systematic uncertainties coming from the data at  $\frac{p}{s} = 1.8 \text{ TeV}$  (see Fig. 2).

## 2.1 FESR (1)

Firstly let us derive the FESR in the spirit of the  $P^0$  sum rule [3]. Let us consider the crossing-even forward scattering amplitude defined by

$$F^{(+)}(\theta) = \frac{f^{pp}(\theta) + f^{pp}(-\theta)}{2} \text{ with } \text{Im } F^{(+)}(\theta) = \frac{k \frac{(+)}{\text{tot}}(\theta)}{4} : \quad (2)$$

We also assume

$$\begin{aligned} \text{Im } F^{(+)}(\theta) &= \text{Im } R(\theta) + \text{Im } F_{p^0}(\theta) \\ &= \frac{1}{M^2} c_0 + c_1 \log \frac{e^i}{M} + c_2 \log^2 \frac{e^i}{M} + \frac{p^0}{M} \frac{1}{M} \end{aligned} \quad ! \quad (3)$$

at high energies ( $\theta > N$ ). We have defined the functions  $R(\theta)$  and  $F_{p^0}(\theta)$  by replacing  $\theta$  by  $M$  in Eq. (3) of ref. [2]. Here,  $M$  is the proton (anti-proton) mass and  $k$  are the incident proton (anti-proton) energy, momentum in the laboratory system, respectively.

Since the amplitude is crossing-even, we have

$$\begin{aligned} R(\theta) &= \frac{i}{2M^2} \left[ 2c_0 + c_2 \log^2 \frac{e^i}{M} + c_1 \log \frac{e^i}{M} + \log \frac{1}{M^A} \right. \\ &\quad \left. + c_2 \log^2 \frac{e^i}{M} + \log^2 \frac{1}{M^A} \right]; \end{aligned} \quad ! \quad (4)$$

$$F_{p^0}(\theta) = \frac{p^0}{M} \left[ \frac{(e^i - M)^{p^0} + (-M)^{p^0}}{\sin \frac{p^0}{M}} \right]^{\frac{1}{A}}; \quad (5)$$

and subsequently obtain

$$\text{Re } R(\theta) = \frac{1}{2M^2} c_1 + 2c_2 \log \frac{1}{M} ; \quad ! \quad (6)$$

$$\text{Re } F_{p^0}(\theta) = \frac{p^0}{M} \frac{1}{M} ; \quad ! \quad 0.5 \quad (7)$$

substituting  $p^0 = \frac{1}{2}$  in Eq. (5). Let us define

$$F^{(+)}(\theta) = F^{(+)}(\theta) - R(\theta) - F_{p^0}(\theta) \quad ! \quad (0) < 0 : \quad (8)$$

Using the similar technique to ref. [2], we obtain

$$\text{Re } F^{(+)}(M) = \frac{2p^0}{0} \frac{\text{Im } F^{(+)}(\theta)}{k^2} d$$

$$\begin{aligned}
&= \frac{2P}{0} \int_0^{Z_M} \frac{1}{k^2} \text{Im } F^{(+)}(d) d + \frac{1}{2} \int_0^{Z_N} \frac{1}{k^2} \text{Im } k^{(+)}_{\text{tot}}(k) dk \\
&\quad \frac{2P}{0} \int_0^{Z_N} \frac{1}{k^2} : \text{Im } R(d) + \frac{P^0}{M} \frac{1}{M} ; d ;
\end{aligned} \quad (9)$$

where  $\bar{N} = \frac{P}{N^2 - M^2}$ ,  $N$ . Let us call Eq. (9) as the FESR (1). If  $c_1, c_2 \neq 0$ , this Eq. (9) reduces to the so-called  $P^0$  FESR in 1962 [3].

## 2.2 FESR (2)

The second FESR corresponding to  $n = 1$  [7] is:

$$\begin{aligned}
&\int_0^{Z_M} \text{Im } F^{(+)}(d) d + \frac{1}{4} \int_0^{Z_N} k^2 \text{Im } k^{(+)}_{\text{tot}}(k) dk \\
&= \int_0^{Z_N} \text{Im } R(d) d + \int_0^{Z_N} \text{Im } F_{P^0}(d) d ;
\end{aligned} \quad (10)$$

We call Eq. (10) as the FESR (2) which we use in our analysis.

## 2.3 The $^{(+)}$ ratio

Let us obtain the  $^{(+)}$  ratio, the ratio of the real to imaginary part of  $F^{(+)}(d)$ , from Eqs. (3), (6) and (7) as

$$\begin{aligned}
^{(+)}(d) &= \frac{\text{Re } F^{(+)}(d)}{\text{Im } F^{(+)}(d)} = \frac{\text{Re } R(d) + \text{Re } F_{P^0}(d)}{\text{Im } R(d) + \text{Im } F_{P^0}(d)} \\
&= \frac{\frac{2M^2}{2M^2} c_1 + 2c_2 \log \frac{M}{\frac{P^0}{M} \frac{1}{M}}}{\frac{k^{(+)}_{\text{tot}}(d)}{4}} ;
\end{aligned} \quad (11)$$

## 2.4 General procedures

The FESR (1) (Eq. (9)) has some problem. i.e., there are the so-called unphysical regions coming from boson poles below the  $pp$  threshold. So, the contributions from unphysical regions of the first term of the right-hand side of Eq. (9) have to be calculated. Reliable estimates, however, are difficult. Therefore, we will not adopt the FESR (1).

On the other hand, contributions from the unphysical regions to the first term of the left-hand side of FESR (2) (Eq. (10)) can be estimated to be an order of 0.1% compared with the second term.<sup>1</sup> Thus, it can easily be neglected.

<sup>1</sup>The average of the imaginary part from boson resonances below the  $pp$  threshold is the smooth extrapolation of the t-channel  $qqqq$  exchange contributions from high energy to  $M$  due to FESR duality [6, 7]. Since  $\text{Im } F_{qqqq}^{(+)}(d) < \text{Im } F^{(+)}(d)$ ,  $\int_0^{R_M} \text{Im } F_{qqqq}^{(+)}(d) d < \int_0^{R_M} \text{Im } F^{(+)}(d) d = \int_0^{R_M} \frac{1}{2} \text{Im } f^{pp}(d) d$

Therefore, the FESR (2) (Eq. (10)), the formula of  $\frac{1}{4} \int_0^{\bar{N}} k^2 \frac{d}{dk} F^{(+)}$  (Eqs. (2) and (3)) and the  $\frac{1}{4} \int_0^{\bar{N}} k^2 \frac{d}{dk} F^{(+)}$  ratio (Eq. (11)) are our starting points. Armed with the FESR (2), we express high-energy parameters  $c_0, c_1, c_2$  in terms of the integral of total cross sections up to  $N$ . Using this FESR (2) as a constraint for  $F^{(+)}$ , the number of independent parameters is three. We then search for the simultaneous best fit to the data points of  $\frac{1}{4} \int_0^{\bar{N}} k^2 \frac{d}{dk} F^{(+)}$  and  $\frac{1}{4} \int_0^{\bar{N}} k^2 \frac{d}{dk} F^{(+)}$  for  $70 \text{ GeV} \leq k \leq 10^6 \text{ GeV}$  to determine the values of  $c_0, c_1, c_2$  giving the least  $\chi^2$ . We thus predict the  $F^{(+)}$  and  $F^{(+)}$  in LHC energy and high-energy cosmic-ray regions.

## 2.5 Data

We use rich data [9] of  $F^{(pp)}$  and  $F^{(p\bar{p})}$  to evaluate the relevant integrals of cross sections appearing in FESR (2). We connect the each data point. We then have

$$\frac{1}{4} \int_0^{\bar{N}} k^2 \frac{d}{dk} F^{(+)}$$
 (12)

for  $\bar{N} = 10 \text{ GeV}$  (which corresponds to  $\bar{s} = E_{cm} = 454 \text{ GeV}$ ). (For more detail about data, see ref. [18].)

It is necessary to pay special attention to treat the data with them maximum  $k = 1.7266 \times 10^6 \text{ GeV}$  ( $\bar{s} = 1.8 \text{ TeV}$ ) in this energy range, which comes from the three experiments E710 [13]–E811 [14] and CDF [15]. The former two experiments are mutually consistent and their averaged  $p\bar{p}$  cross section is  $\frac{pp}{tot} = 72.0 \pm 1.7 \text{ mb}$ , which deviates from the result of CDF experiment  $\frac{pp}{tot} = 80.03 \pm 2.24 \text{ mb}$ .

The two points of  $F^{(pp)}$  are reported in the SPS and Tevatron-collider energy region,  $1 \leq 10^5 \text{ GeV} \leq k \leq 2 \times 10^6 \text{ GeV}$  (at  $k = 1.5597 \times 10^5 \text{ GeV}$  ( $\bar{s} = 541 \text{ GeV}$ ) [17] and  $k = 1.7266 \times 10^6 \text{ GeV}$  ( $\bar{s} = 1.8 \text{ TeV}$ ) [13]). We regard these two points as the  $F^{(+)}$  data. As a result, we obtain 9 points of  $F^{(+)}$  up to Tevatron-collider energy region,  $70 \text{ GeV} \leq k \leq 10^6 \text{ GeV}$ .

In the actual analyses, we use  $\text{Re } F^{(+)}$  instead of  $F^{(+)}$  ( $= \text{Re } F^{(+)}/\text{Im } F^{(+)}$ ). The data points of  $\text{Re } F^{(+)}$  ( $k$ ) are made by multiplying  $F^{(+)}$  ( $k$ ) by  $\text{Im } F^{(+)}$  ( $k$ ) =  $\frac{k}{8} (\frac{pp}{tot} (k) + \frac{pp}{tot} (k))$ .

---

$\frac{M^2}{4} \text{Im } f^{pp} \Big|_{k=0} = 3.2 \text{ GeV} \quad \frac{1}{4} \int_0^{\bar{N}} k^2 \frac{d}{dk} F^{(+)}$  ( $k$ )  $dk = 3403 \pm 20 \text{ GeV}$ , where we use the experimental value,  $\frac{k}{4} \frac{pp}{tot} \Big|_{k=0} = 14.4 \text{ GeV}^{-1}$  in  $k < 0.3 \text{ GeV}$ . So, resonance contributions to the first term of Eq. (10) is less than 0.1% of the second term.

Besides boson resonances, there may be additional contributions from multipion contributions below  $p\bar{p}$  threshold. In the  $p\bar{p}$  annihilation,  $p\bar{p} \rightarrow \pi^+ \pi^-$  could give comparable contributions with  $\pi^0$  meson, but multipion contributions are suppressed due to the phase volume effects. Therefore, the first term of Eq. (10) will still be negligible even if the above contributions are included.

Table 1: The values of  $\chi^2$  for the  $t_1$  ( $t$  up to ISR energy) and the  $t_2$  and  $t_3$  ( $t$ s up to Tevatron-collider energy).  $N_F$  and  $N$  ( $N$ ) are the degree of freedom and the number of  $^{(+)}$  data points in the fitted energy region.

	$\chi^2 = N_F$	$\chi^2 = N$	$\chi^2 = N$
$t_1$	10.6/15	3.6/12	7.0/7
$t_2$	16.5/23	8.1/18	8.4/9
$t_3$	15.9/23	9.0/18	6.9/9

## 2.6 Analysis

As was explained in the general procedure, both  $\chi^2_{tot}^{(+)}$  and  $R_{eF}^{(+)}$  data in 70GeV  $\mathbf{k}$   $P_{large}$  are fitted simultaneously through the formula Eq. (3) and Eq. (11) with the FESR (2) (Eq. (10)) as a constraint. FESR (2) with Eq. (12) gives us

$$8.87 = c_0 + 2.04c_1 + 4.26c_2 + 0.367_{p^0}; \quad (13)$$

which is used as a constraint of  $p^0 = p^0(c_0; c_1; c_2)$ , and the fitting is done by three parameters  $c_0; c_1$  and  $c_2$ .

We have done for the following three cases:

t 1): The fit to the data up to ISR energy region, 70GeV  $\mathbf{k}$  2100GeV, which includes 12 points of  $\chi^2_{tot}^{(+)}$  and 7 points of  $\chi^2_{p^0}^{(+)}$ .

t 2): The fit to the data up to Tevatron-collider energy region, 70GeV  $\mathbf{k}$   $2 \cdot 10^6$ GeV. For  $\mathbf{k} = 1.7266 \cdot 10^6$ GeV ( $\sqrt{s} = 1.8$ TeV), the E710=E811 datum is used. There are 18 points of  $\chi^2_{tot}^{(+)}$  and 9 points of  $\chi^2_{p^0}^{(+)}$ .

t 3): The same as t 2, except for the CDF value at  $\sqrt{s} = 1.8$ TeV, are used.

## 2.7 Results of the $t$

The results are shown in Fig. 1 (Fig. 2) for the  $t_1$  ( $t_2$  and  $t_3$ ). The  $\chi^2$ -d.o.f are given in Table 1. The reduced  $\chi^2$  and the respective  $\chi^2$ -values devided by the number of data points for  $\chi^2_{tot}^{(+)}$  and  $\chi^2_{p^0}^{(+)}$  are less than or equal to unity. The  $t$ s are successful in all cases. There are some systematic differences between  $t_2$  and  $t_3$ , which come from the experimental uncertainty of the data at  $\sqrt{s} = 1.8$ TeV mentioned above.

The best- $t$  values of the parameters are given in Table 2. Here the errors of one standard deviation are also given.

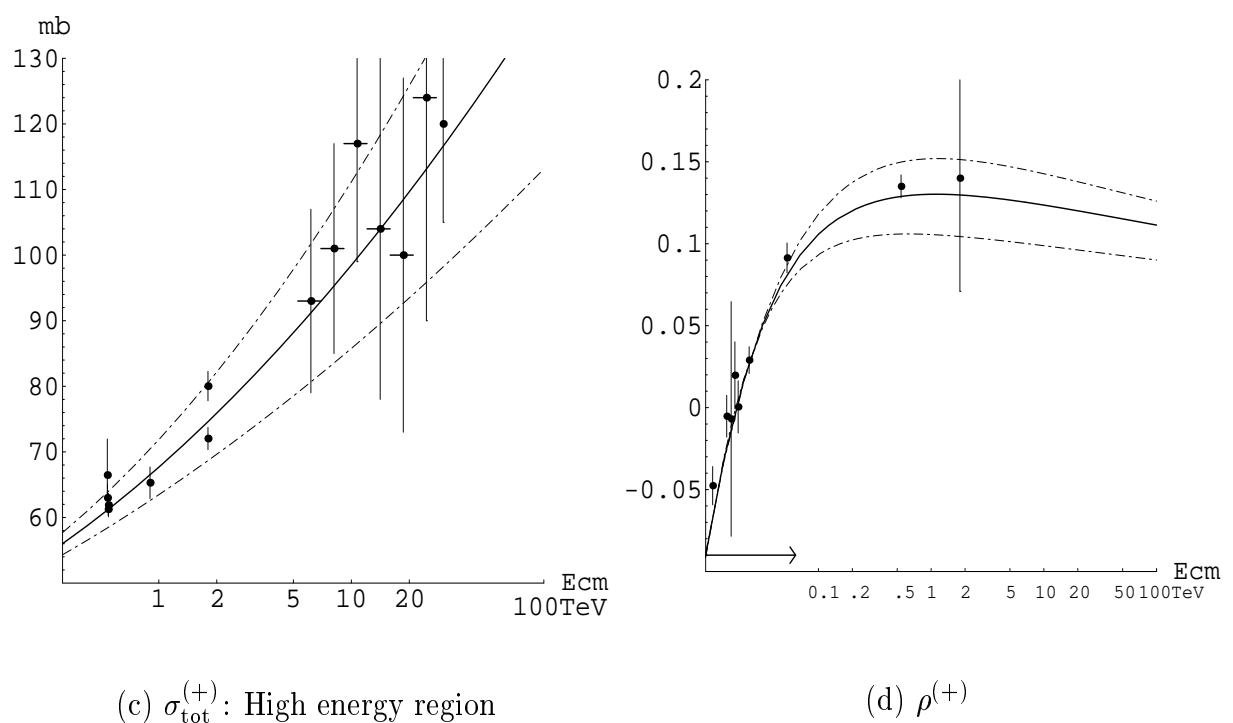
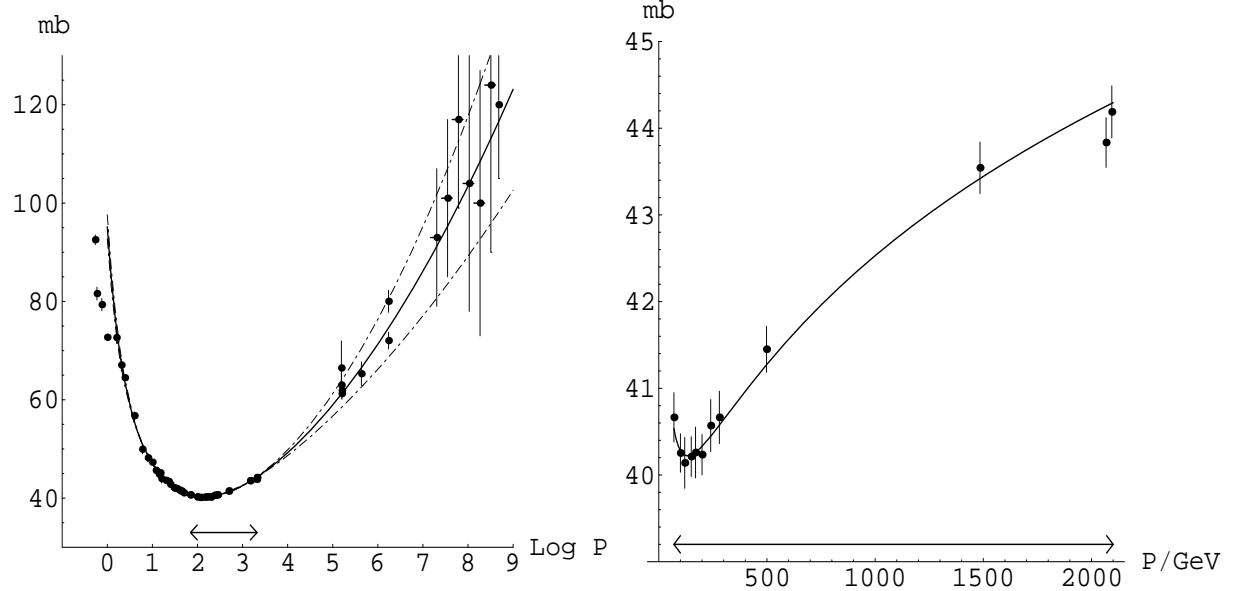
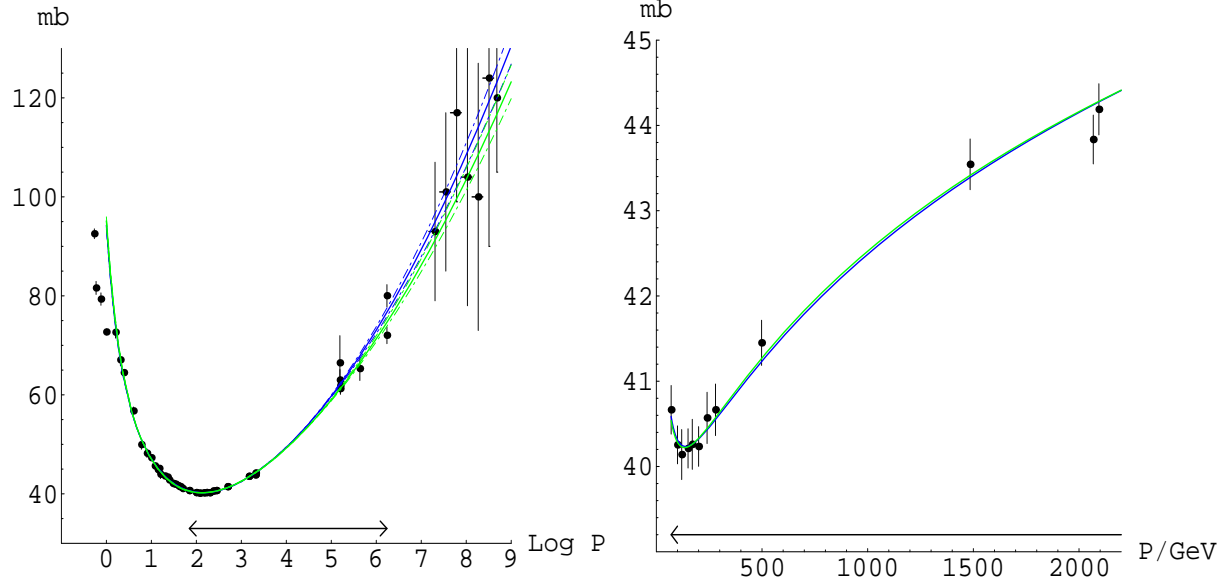
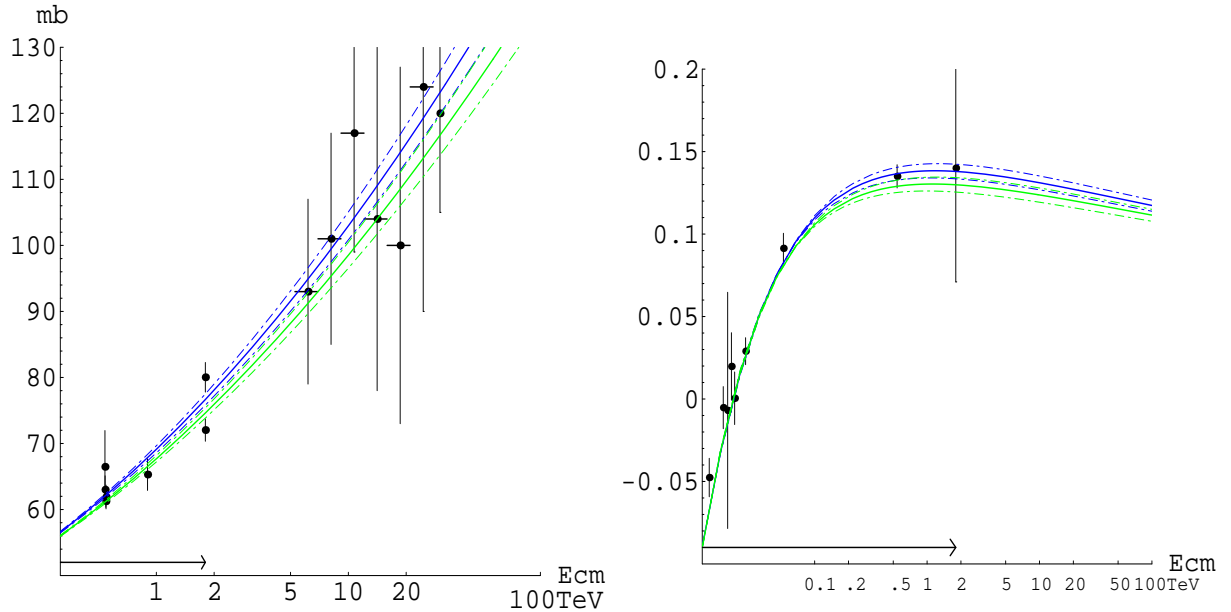


Figure 1: Predictions for  $\rho^{(+)}$  and  $\sigma_{\text{tot}}^{(+)}$  in terms of the  $t$ . The  $t$  is done for the data up to the ISR energy, in the region  $70 \text{ GeV} \leq P_{\text{lab}} \leq 2100 \text{ GeV}$  ( $11.5 \text{ GeV} \leq \sqrt{s} \leq 62.7 \text{ GeV}$ ) which is shown by the arrow in each figure. Total cross section  $\sigma_{\text{tot}}^{(+)}$  in (a) all energy region, versus  $\log_{10} P_{\text{lab}} = G \text{ eV}$ , (b) low energy region (up to ISR energy), versus  $P_{\text{lab}} = G \text{ eV}$  and (c) high energy (Tevatron-collider, LHC and cosmic-ray energy) region, versus center of mass energy  $E_{\text{cm}}$  in TeV unit. (d) gives the  $\rho^{(+)}$  ( $= \text{Re } F^{(+)} = \text{Im } F^{(+)}$ ) in high energy region, versus  $E_{\text{cm}}$  in terms of TeV. The thin dot-dashed lines represent the one standard deviation.



(a)  $\sigma_{\text{tot}}^{(+)}$ : All region

(b)  $\sigma_{\text{tot}}^{(+)}$ : Low energy region



(c)  $\sigma_{\text{tot}}^{(+)}$ : High energy region

(d)  $\rho^{(+)}$

Figure 2: Predictions for  $\rho^{(+)}$  and  $\sigma_{\text{tot}}^{(+)}$  in terms of the  $t_2$  (shown by green lines) and  $t_3$  (shown by blue lines). The  $t$  is done for the data up to Tevatron-collider energy, in the region  $70 \text{ GeV} \leq p_T \leq 10^6 \text{ GeV}$  ( $\sqrt{s} = 1.8 \text{ TeV}$ ) which is shown by the arrow. For  $k = 1:7266 \cdot 10^6 \text{ GeV}$  ( $\sqrt{s} = E_{\text{cm}} = 1.8 \text{ TeV}$ ), the averaged datum of E710 [13]/E811 [14],  $\sigma_{\text{tot}}^{\text{pp}} = 72.0 \pm 1.7 \text{ mb}$ , is used in  $t_2$ , while the  $\sigma_{\text{tot}}^{\text{pp}} = 80.03 \pm 2.24 \text{ mb}$  of CDF [15] is used in  $t_3$ . For each figure, see the caption in Fig.1.

Table 2: The best- $t$  values of parameters in the  $t_1$ ,  $t_2$  and  $t_3$ .

	$c_2$	$c_1$	$c_0$	$p^0$
$t_1$	0.0411	0.0199	0.074	0.287
$t_2$	0.0412	0.0041	0.076	0.069
$t_3$	0.0484	0.0043	0.181	0.071
	5.92	1.07	7.96	1.55
	0.28	0.29	7.95	0.44
	6.33	0.29	7.37	0.45

Table 3: The predictions of  $\frac{p^+}{s} = E_{cm} = 14\text{TeV}$  ( $P_{lab} = 1.04 \cdot 10^8 \text{GeV}$ ), and at a very high energy  $P_{lab} = 5 \cdot 10^{20} \text{eV}$  ( $\frac{p^+}{s} = E_{cm} = 967\text{TeV}$ ) in cosm ic-ray region.

	$\frac{p^+}{s} = 14\text{TeV}$	$\frac{p^+}{s} = 14\text{TeV}$	$\frac{p^+}{s} = 5 \cdot 10^{20} \text{eV}$	$\frac{p^+}{s} = 5 \cdot 10^{20} \text{eV}$
$t_1$	103.8	14.3mb	0.122 $\pm 0.018$	188 $\pm 0.024$
$t_2$	103.8	2.3mb	0.122 $\pm 0.004$	189 $\pm 0.004$
$t_3$	108.9	2.4mb	0.129 $\pm 0.004$	204 $\pm 0.004$

### 3 Predictions for $\frac{p^+}{s}$ and $\frac{p^+}{s}$ at LHC and Cosm ic-ray Energy Region

By using the values of parameters in Table 2, we can predict the  $\frac{p^+}{s}$  and  $\frac{p^+}{s}$  in higher energy region, as are shown, respectively in (c) and (d) of Fig. 1 and 2. The thin dot-dashed lines represent the one standard deviation.

As is seen in (c) and (d) of Fig. 1, the  $t_1$  leads to the prediction of  $\frac{p^+}{s}$  and  $\frac{p^+}{s}$  with somewhat large errors in the Tevatron-collider energy region, although the best- $t$  curves are consistent with the present experimental data in this region. Furthermore, the predicted values of  $\frac{p^+}{s}$  agree with pp experimental data at the cosm ic-ray energy regions [8, 21] within errors (see (a), (c) of Fig. 1). The best- $t$  curve gives  $\chi^2 = (\text{number of data})$  to be 13.0/16, and the prediction is successful. As was mentioned before, it has to be noted that the energy range of predicted  $\frac{p^+}{s}$  is several orders of magnitude larger than the energy region of the  $\frac{p^+}{s}$ ,  $\frac{p^+}{s}$  input. If we use data up to Tevatron-collider energy region as in the  $t_2$  and  $t_3$ , the situation is much improved (see (a), (c) of Fig. 2), although there is systematic uncertainty depending on the treatment of the data at  $\frac{p^+}{s} = 1.8\text{TeV}$ .

The best- $t$  curve gives  $\chi^2 = (\text{number of data})$  from cosm ic-ray data, 1.3/7 (1.0/7) for  $t_2$  ( $t_3$ ).

We can predict the values of  $\frac{p^+}{s}$  and  $\frac{p^+}{s}$  at LHC energy,  $\frac{p^+}{s} = E_{cm} = 14\text{TeV}$  and at very high energy of cosm ic-ray region. The relevant energies are very high, and the  $\frac{p^+}{s}$  and  $\frac{p^+}{s}$  can be regarded to be equal to the  $\frac{pp}{s}$  and  $\frac{pp}{s}$ . The results are shown in Table 3.

The prediction by the  $t_1$  in which data up to the ISR energy are used as input has somewhat large (fairly large) errors at LHC energy (at high energy of cosmic ray). By including the data up to the Tevatron collider, the prediction of  $t_2$  (using E710/E811 datum) is smaller than that of  $t_3$  (using CDF datum). We regard the difference between the results of  $t_2$  and  $t_3$  as the systematic uncertainties of our predictions. As a result, we predict

$$\frac{pp}{tot} = 106.3 \pm 5.1_{\text{syst}} \pm 2.4_{\text{stat}} \text{ mb}; \quad \frac{pp}{s} = 0.126 \pm 0.007_{\text{syst}} \pm 0.004_{\text{stat}} \quad (14)$$

at LHC energy ( $\frac{p}{s} = E_{cm} = 14 \text{ TeV}$ ). We obtain fairly large systematic errors coming from the experimental uncertainty at  $\frac{p}{s} = 1.8 \text{ TeV}$ .

## 4 Comparison with Other Groups

The predicted central value of  $\frac{pp}{tot}$  is in good agreement with Block and Halzen [5]  $\frac{pp}{tot} = 107.4 \pm 1.2 \text{ mb}$ ,  $\frac{pp}{s} = 0.132 \pm 0.001$ . In contrary to our results (see Fig. 2(a), (c)), however, their values are not affected so much about CDF, E710/E811 discrepancy. In our case, the measurements at LHC energy will discriminate which solution is better at Tevatron. Our prediction has also to be compared with Cudell et al [22]  $\frac{pp}{tot} = 111.5 \pm 1.2_{\text{syst}}^{+4.1}_{-2.1_{\text{stat}}}$  mb,  $\frac{pp}{s} = 0.1361 \pm 0.0015_{\text{syst}}^{+0.0058} \pm 0.0025_{\text{stat}}$ , who's fitting techniques favour the CDF point at  $\frac{p}{s} = 1.8 \text{ TeV}$ , which leads to large value for  $\frac{pp}{tot}$ . The LHC measurements would also clarify which is the best solution among the three high-energy cosmic-ray samples [19, 20, 21].

**Acknowledgements** One of the authors (K.I.) would like to thank Prof. M. Nishimura and Prof. H. Kawai for their kind hospitality for completing this work, and also to Prof. L. Jenkovszky and the Organizing Committee for giving an opportunity to present this talk. This work is supported by Grant-in-Aid for Scientific Research on Priority Areas, Number of Area 763 "Dynamics of Strings and Fields", from the Ministry of Education of Culture, Sports, Science and Technology, Japan.

## References

- [1] M. Froissart, Phys. Rev. 123 (1961) 1053.  
A. Martin, Nuovo Cim. 42 (1966) 930.
- [2] K. Igi and M. Ishida, Phys. Rev. D 66 (2002) 034023.
- [3] K. Igi, Phys. Rev. Lett. 9 (1962) 76.

[4] M .M .B lock and F .H alzen, Phys. Rev. D 70 (2004) 091901.

[5] M .M .B lock and F .H alzen, hep-ph/0506031.

[6] K .I gi and S.M atsuda, Phys. Rev. Lett. 18 (1967) 625.

[7] R .D olen, D .H orn and C .S chmid, Phys. Rev. 166 (1968) 1768. This paper includes references on earlier papers on FESR .

[8] M .H onda et al., Phys. Rev. Lett. 70 (1993) 525.  
R .M .B altrusaitis et al., Phys. Rev. Lett. 52 (1984) 1380.

[9] Particle D ata G roup, S .E idehn et al., Phys. Lett. B 592 (2004) 313.

[10] G .C arboni et al., Nucl. Phys. B 254 (1984) 697.  
U .A maldi et al., Nucl. Phys. B 145 (1978) 367.

[11] G .A mison et al., UA 1 C ollaboration, Phys. Lett. B 128 (1983) 336.  
R .B attiston et al., UA 4 C ollaboration, Phys. Lett. B 117 (1982) 126.  
M .B ozzo et al., UA 4 C ollaboration, Phys. Lett. B 147 (1984) 392.  
G .J .A lner et al., UA 5 C ollaboration, Zeit. Phys. C 32 (1986) 153.

[12] C .A ugier et al., Phys. Lett. B 344 (1995) 451.

[13] N .A .A mos et al., E -710 C ollaboration, Phys. Rev. Lett. 68 (1992) 2433.

[14] C .A vila et al., E -811 C ollaboration, Phys. Lett. B 445 (1999) 419.

[15] F .A be et al., CDF C ollaboration, Phys. Rev. D 50 (1994) 5550.

[16] N .A mos et al., Nucl. Phys. B 262 (1985) 689.

[17] C .A ugier et al., Phys. Lett. B 316 (1993) 448.

[18] K .I gi and M .I shida, Phys. Lett. B 622 (2005) 286.

[19] T .K .G aisser et al., Phys. Rev. D 36 (1987) 1350

[20] N .N .N ikolaev, Phys. Rev. D 48 (1993) R1904.

[21] M .M .B lock et al., Phys. Rev. D 62 (2000) 077501.

[22] J .R .C udell et al., Phys. Rev. Lett. 89 (2002) 201801.